Revisiting Gray Pixel for Statistical Illumination Estimation

Yanlin Qian[1,3], Said Pertuz[1], Jarno Nikkanen[2], Joni-Kristian Kämäräinen[1] and Jiri Matas[3]

[1]*Laboratory of Signal Processing, Tampere University of Technology, Finland*

[2]*Intel Finland, Finland*

[3]*Center for Machine Perception, Czech Technical University in Prague, Czech Republic*

Keywords: Illumination Estimation, Color Constancy, Gray Pixel.

Abstract: We present a statistical color constancy method that relies on novel gray pixel detection and mean shift clustering. The method, called Mean Shifted Grey Pixel – MSGP, is based on the observation: true-gray pixels are aligned towards one single direction. Our solution is compact, easy to compute and requires no training. Experiments on two real-world benchmarks show that the proposed approach outperforms state-of-the-art methods in the camera-agnostic scenario. In the setting where the camera is known, MSGP outperforms all statistical methods.

1 INTRODUCTION

The human eye automatically adapts to changes in imaging conditions and illumination of the scenes. Analogously, the ability of making color images look natural regardless of changing illumination is known as *color constancy* and is an important feature of consumer digital cameras in order to yield visually canonical images. Color constancy is an important step in different computer vision applications, such as fine-grained classification, semantic segmentation, scene rendering and object tracking, among others (Foster, 2011).

For decades, the classical approaches for color constancy in digital cameras, *statistical methods*, have relied on the assumption that some global or local statistical properties of the illumination are constant and can therefore be estimated directly from the image (Brainard and Wandell, 1986; Barnard et al., 2002; Van De Weijer et al., 2007; Finlayson and Trezzi, 2004; Gao et al., 2014; Yang et al., 2015; Cheng et al., 2014). This approach has the advantage of being independent to the acquisition device since the properties of the scene illumination are estimated in a per-image basis. Recently, state-of-the-art methods including convolutional neural networks (CNN), namely *learning-based methods* (Chakrabarti et al., 2012; Gijsenij et al., 2010; Gehler et al., 2008; Gijsenij and Gevers, 2011; Joze and Drew, 2014), have consistently outperformed statistical methods when validated in several mainstream benchmarks. We argue that learning-based methods depend on the assumption that the statistical distribution of the illumination in both the training and testing images is similar. In other words, learning-based methods assume that imaging and illumination conditions of a given image can be inferred from previous training examples, thus becoming heavily dependent on the training data (Gao et al., 2017).

In order to assess the limitation of color constancy methods to cope with differences between training and testing images, we focus on the *Camera-agnostic color constancy* setting. For illustration, consider the case when a user retrieves an image from the unknown camera[1] and wants to color correct it. In this scenario, in which very little is known about the camera or capturing process of the image, color correction must be performed without strong assumptions on the source of the image or imaging device. In this less researched but still important setting, we experimentally show that, in camera-agnostic color constancy, learning-based methods perform poorly compared to statistical methods. As a result, there is a need for approaches that are insensitive to parameters such as the camera or imaging process used to capture the image.

In this paper we propose a new statistical color constancy method. The proposed method, cal-

---

[1]We assume the image is with linear response and calibrated black offset, where color constancy method should be applied. Note that images over web are not usually this case.

Figure 1: Detection of gray pixels. From left to right: input image, color-corrected image using ground-truth, pixels chosen by the proposed method in Section 4.3, and pixels chosen by (Yang et al., 2015). Macbeth Color Checker are masked out due to both methods find gray pixels on gray regions.

led *mean-shifted gray pixel*, or MSGP, is a process that detects pixels that are assumed to be gray under neutral illumination. Why gray pixels? Gray or nearly gray pixels are wide spread in indoor and outdoor images (Yang et al., 2015). In the process of manufacturing camera, each camera is calibrated to maintain: *gray pixels will be rendered gray in linear image (not raw response) under standard neutral illumination*. Gray pixel examples are shown in the third column in Fig. 1.

Considering that gray pixels are informative *w.r.t.* casting illumination, it is possible to transform the scene illumination estimation task into gray pixel detection. This paper proposes an accurate method for the detection of gray pixels by combining a novel *grayness measure* with Mean-shift clustering in color space.

Experimental results in camera-agnostic color constancy show that the proposed algorithm outperforms both statistical and learning-based methods of the state-of-the-art. Even in the non camera-agnostic scenario, *i.e.* using k-fold cross validation in the same datasets, the proposed method outperforms other statistical methods and shows a competitive performance when compared to learning-based methods.

2 PREVIOUS RELATED WORK

Assuming a photometric linear image I captured using a digital camera, with pixels below black level and above saturation level corrected, the simplified imaging formation under one global illumination source can be expressed as (Gijsenij et al., 2011):

$$I_i(x,y) = \int L(\lambda)S_i(\lambda)R(x,y,\lambda)d\lambda, i \in \{R,G,B\}, \quad (1)$$

where $I_i(x,y)$ is the measured image color value at spatial location (x,y), $L(\lambda)$ the wavelength distribution of the global light source, $S_i(\lambda)$ the spectral response of the color sensor, $R(x,y,\lambda)$ the surface reflectance and λ the wavelength.

Under the narrow-band assumption (Von Kries coefficient law (von Kries, 1970)), Eq. 1 can be further simplified as (same as (Barron, 2015)):

$$I = WL, \quad (2)$$

which shows that the whole captured image I is the element-wise Hadamard product of the white-balanced image W and the illumination L.

The *goal* of all color constancy methods, both learning-based and statistical methods, is to estimate L, so as to recover W, given I.

Learning-based Methods (Chakrabarti et al., 2012; Gijsenij et al., 2010; Gehler et al., 2008; Gijsenij

and Gevers, 2011; Joze and Drew, 2014; Qian et al., 2016; Qian et al., 2017) aim at building a model that relates the captured image I and the sought illumination L from extensive training data. Among the best-performing state-of-the-art approaches, the CCC method discriminatively learns convolutional filters in a 2D log-chroma space (Barron, 2015). This framework was subsequently accelerated using the Fast Fourier Transform on a chroma torus (Barron and Tsai, 2017). Chakrabarti *et al.* (Chakrabarti, 2015) leverage the normalized luminance for illumination prediction by learning a conditional chromaticity distribution. DS-Net (Shi et al., 2016) and FC[4] Net (Hu et al., 2017) are two representative methods using deep learning. The former network chooses an estimate from multiple illumination guesses using a two-branch CNN architecture, while the later addresses local estimation ambiguities of patches using a segmentation-like framework. Learning-based methods achieve great success in predicting pre-recorded "ground-truth" illumination color to a fairly high accurate level, but heavily depending on the same cameras being used in both training and testing images (see Sections 3 and 5.2). The Corrected-Moment method (Finlayson, 2013) can also be considered as a learning-based method as it needs to train a corrected matrix for each dataset.

Statistical Methods estimate illumination by making some assumptions about the local or global regularity of the illumination and reflectance of the input image. The simplest such method is *Gray World* (Buchsbaum, 1980), that assumes that the global average of reflectance is achromatic. The generalization of this assumption by restricting it to local patches and higher-order gradients has led to some classical and recent statistics-based methods, such as White Patch (Brainard and Wandell, 1986), General Gray World (Barnard et al., 2002), Gray Edge (Van De Weijer et al., 2007), Shades-of-Gray (Finlayson and Trezzi, 2004) and LSRS (Gao et al., 2014), among others (Cheng et al., 2014). The closest works to ours are Xiong *et al.* (Xiong et al., 2007) and Gray Pixel (Yang et al., 2015). Xiong *et al.* (Xiong et al., 2007) finds gray surfaces based on a special LIS space, but this method is camera-dependent. The Gray Pixel method will be discussed in Section 4.

Physics-based and other Methods (Tominaga, 1996; Finlayson and Schaefer, 2001a; Finlayson and Schaefer, 2001b) estimate illumination from the understanding of the physical process of image formation (*e.g.* the Dichromatic Model), thus being able to model highlights and inter-reflections. Most physics-based methods estimate illumination based on intersection of multiple dichromatic lines, making them work well

on toy images and images with only a few surfaces but not very reliable on natural images (Finlayson and Schaefer, 2001b). The latest physics-based method is (Woo et al., 2018), which relies on the longest dichromatic line segment assuming Phong reflection model holds and an ambient light exists. Although our method is based on the Dichromatic Model, we classify our approach as *statistical* since the core of the method is finding gray pixels based on some observed image statistics. We refer readers to (Gijsenij et al., 2011) for more details about physics-based methods. The **contribution** of this paper is three-fold:

- We experimentally demonstrate that, in the camera-agnostic color constancy setting, state-of-the-art learning-based methods are outperformed by statistical methods
- We point out the hidden elongated pixel prior over indoor and outdoor color constancy datasets.
- We present the Mean-shift-based Gray Pixel method, robustly searching dominant illumination (mode) and achieving state-of-the-art performance among competing training-free alternatives. Code will be released upon publication.

3 CAMERA-AGNOSTIC COLOR CONSTANCY

For a given camera, noted as C, Eq. 2 can be rewritten as:

$$I_C = W_C L_C, \qquad (3)$$

which indicates that both, the captured image I_C, the canonical image W_C and the illumination L_C that we need to estimate, are dependent on the camera type C. W_C indicates that in canonical light, the images captured by different cameras of the same scene differ.

The color constancy problem in learning-based methods can be stated as $\tilde{L}_C = f(w, I_C)$, where $\tilde{L}_C$ is the estimated illumination, and $f(w, \cdot)$ is the mapping to be learned with parameters w. The mapping $f(w, \cdot)$ can be embodied by various machine learning models or an ensemble of them. If the learning process for a particular dataset is guided by the distance (*e.g.* angular error) between $\tilde{L}_C$ and L_C, w will undoubtedly be biased by the particular characteristics of the camera C. In other words, the parameters of $f(w, \cdot)$ will be learned to be "well-performing" on a specific dataset that encompasses one or a few pre-selected cameras. With the massive modeling capability of some machine learning models (*e.g.* regression trees and deep learning), the camera sensibility function of a bag of cameras can be modeled up to a high degree. In the literature, the validation of color constancy methods is

customarily performed using k-fold cross-validation on the same dataset. As a result, this validation process favors learning-based methods and fails to assess their performance for color correction in images from an unknown camera (Gao et al., 2017).

In this work, we define *camera-agnostic color constancy* as the problem of estimating the illumination L_C of a color-biased image I_C that has been captured by a camera C of unknown properties. For learning-based methods, this implies that the input image I_C has been captured by a camera not previously "seen" in the training process. Therefore, a rigorous validation process of color constancy algorithms should consider both, camera-agnostic and known-camera scenarios. By leveraging publicly available datasets, this can be achieved by training in one dataset and testing in other without overlapping cameras (see Section 5). In contrast to learning-based methods, statistical methods have the advantage of adjusting the model in a per-image basis thus having the potential to implicitly deal with the camera-agnostic problem.

4 MEAN-SHIFTED GRAY PIXEL

The proposed mean-shifted gray pixel algorithm, or MSGP, is built on the assumption that achromatic pixels in the corresponding canonical image can be used to estimate the global illumination. Specifically, achromatic pixels are visually gray in the color corrected image. Yang *et al.* (Yang et al., 2015) claimed the mentioned assumption, and experimentally demonstrated the presence of detectable gray pixels in most natural scenes under white light. In this work, we further extend the concept of the Gray Pixel method by means of an adaptive method for the detection gray pixels that combines a new grayness function and mean-shift clustering.

4.1 Original Gray Pixel (GP) Revisited

In this section, we revisited the original Gray Pixel method (Yang et al., 2015), which is derived from a limited diffuse reflection model. Applying a log transformation to both sides of (2), we have:

$$\log(I_i^{(x,y)}) = \log(W_i^{(x,y)}) + \log(L_i) \qquad (4)$$

In a small enough local neighborhood, the illumination L can be assumed as uniform under global illumination constrains. As a result, the application of a linear channel-wise local contrast operator $C\{\cdot\}$

(Laplacian of Gaussian, which we will use for the remainder of the paper) on (4) yields:

$$C\{\log(I_i^{(x,y)})\} = C\{\log(W_i^{(x,y)})\} \qquad (5)$$

Eq. (5) indicates a well-known observation: the casting illumination is irrelevant to the channel-wise local contrast of a small local neighborhood (Geusebroek et al., 2001). It also means that regions with no contrast are useless for obtaining illumination cues. Following (Yang et al., 2015), with balanced R, G and B responses, the following condition must be met by gray pixels:

$$C\{\log(I_R^{(x,y)})\} = C\{\log(I_G^{(x,y)})\} = C\{\log(I_B^{(x,y)})\} \neq 0. \qquad (6)$$

In practice, (6) does not hold strictly. As a result, it is necessary to propose a "grayness" measure in order to detect nearly gray pixels. For the sake of simplicity, let us define the local contrast of a log-transformed image pixel located at (x,y) as $\Delta_i(x,y) = C\{\log(I_i^{(x,y)})\}$ with $i \in \{R,G,B\}$. In (Yang et al., 2015), the grayness measure of a pixel, $G(x,y)$, is defined as:

$$G(x,y) = \left(\frac{1}{3} \sum_{i \in \{R,G,B\}} \frac{(\Delta_i(x,y) - \bar{\Delta}(x,y))^2}{\bar{\Delta}(x,y)} \right)^{1/2}, \qquad (7)$$

where $\bar{\Delta}(x,y)$ is the average of channels R, G and B.

It is claimed that the smaller $G(x,y)$ is, the more gray a pixel is under white light. Then some post-processing steps are applied to weaken dark pixels (luminance as dominator) and isolated pixels (local averaging), for which we refer readers to the original GP (Yang et al., 2015).

A major drawback of Eq. 7 is that the grayness estimate depends on the luminance of the pixels. Specifically, the effect of $\bar{\Delta}$ results in gray pixels having different grayness values due to differences in luminance. Alternatively, we propose that grayness should only depend on *chromaticity*. Therefore, in the next section, we will introduce a new grayness function to replace Eq. 7.

4.2 Grayness Function

We propose an ideal grayness function $G(\cdot) \in [0,1]$ where 0 denotes pure gray of a pixel color. Without specification, the grayness function works in RGB space as it is closest to the image formation process and main choice of in line of research (Yang et al., 2015; Barron and Tsai, 2017). Our grayness function should comply with the following properties:

Property 1	$G(\cdot)$ is invariant to the luminance (sum of RGB values).
Property 2	$G(\cdot)$ outputs monotonically decreasing value for increasing visual grayness, *e.g.* from red to white.
Property 3	Pure gray pixels (on the black-to-white line) should be have value 0.

In addition the three above-mentioned properties, it is also desirable that the output space of the grayness function be normalized (so that no subsequent normalization is required), as well as having a physical meaning so that it can be used for other computer vision tasks. Alternatively to the grayness measure proposed in (Yang et al., 2015), we propose a new grayness measure based on the angular error function that complies with all these properties:

$$G(x,y) = \cos^{-1}\left(\frac{\langle \Delta(x,y),\mathbf{g}\rangle}{\|\Delta(x,y)\|\|\mathbf{g}\|_2}\right), \qquad (8)$$

where $\Delta(x,y) = [\Delta_r, \Delta_g, \Delta_b]^\mathsf{T}$ is the RGB vector in location (x,y), $\mathbf{g}$ is the gray light reference vector $[g_r, g_g, g_b]^\mathsf{T}$, and $\|\cdot\|_n$ refers to the ℓn norm.

Our motivation behind Eq. 8 is that, even in the color-biased scenario, it is possible to assume that all gray colors captured by the same camera will have balanced R, G, B components, regardless of their luminance level. As a result, it is possible to assess their grayness level by measuring the angular error with respect to a reference gray value. Notice that, in general, the gray reference vector $\mathbf{g}$ can have spatially-varying values in order to adjust for changes in the illumination of the scene. In this work, however, we assume that the global illumination source remains constant in the scene and adopt the canonical gray value as reference: $\mathbf{g} = [1,1,1]^\mathsf{T}$. In this case, Eq. 8 can be further simplified as:

$$G(x,y) = \cos^{-1}\left(\frac{1}{\sqrt{3}}\frac{\|\Delta(x,y)\|_1}{\|\Delta(x,y)\|_2}\right), \qquad (9)$$

Eq. 9 measures how gray a pixel is, using the angular distance from the local contrast vector to the gray light $\mathbf{g}$, thus meeting Properties 1 and 2. When the point (x,y) is completely gray, $G(x,y)$ is 0 and increases monotonically with decreasing level of grayness, thus meeting Property 3. In addition, the output ranges from $0°$ to $\cos^{-1}(\frac{1}{\sqrt{3}})$ for each image, thus being normalized.

Empirical Evidence – The next question is whether this new grayness function brings different ordering of pixels according to their grayness levels. To answer this, we replace Eq. 7 with Eq. 8 in the original GP algorithm and estimate illumination in two mainstream color constancy benchmarks where GP is evaluated. Table 1 shows the performance improvement

by a large margin ($0.6°$ reduction in median error for SFU Color Checker) when we use the proposed grayness measure Eq. 8. Results on the SFU Indoor dataset do not differ much, arguably because the dataset is collected in a laboratory environment with a restricted set-up (many image feel artificial and examples are shown in Fig 2). The proposed method is based on the assumption of natural image statistics and works for more general cases. For the results shown in Table 1, the top 0.1% pixels with G values are chosen as gray pixels, as recommended by (Yang et al., 2015). The local contrast operator $C\{\cdot\}$ is the Laplacian of Gaussian.

Table 1: Angular error of the Gray Pixel (Yang et al., 2015) algorithm with different grayness functions: original grayness function (GP) and proposed grayness function in Eq. 9 (GP*).

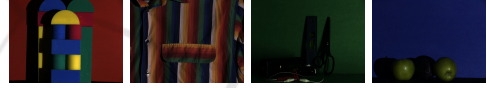|	SFU Color Checker			SFU Indoor		
	Mean	Med	Trimean	Mean	Med	Trimean
GP	4.6	3.1	–	5.3	2.3	–
GP*	4.1	2.5	2.8	5.3	2.2	2.7

Figure 2: Examples of SFU Indoor dataset.

Here we mathematically analyze the connection between the grayness function in Eq. 7 and the proposed grayness measure in Eq. 9. To avoid readers' confusion, we term the original grayness measure in Eq. 7 as $G_\sigma(x,y)$ and the proposed grayness function of Eq. 8 as $G_\theta(x,y)$. In the sequel, we demonstrate that G_σ and G_θ are related by:

$$G_\sigma(x,y) = \gamma(x,y)G_\theta(x,y), \qquad (10)$$

where $\gamma(x,y)$ is a luminance-dependent term.

In order to demonstrate the relationship in Eq. 10, we approximate G_θ as follows[2]:

$$G_\theta \approx \sqrt{1 - \frac{1}{\sqrt{3}}\frac{\|\Delta\|_1}{\|\Delta\|_2}} \qquad (11)$$

It can be readily shown that Eq. 11 is an approximation of the same order of Eq. 9 in the interval $[0,1]$. With this approximation, G_θ and G_σ can be rewritten as:

$$3\beta G_\sigma^2 = \alpha^2 - 3\beta^2 \qquad (12)$$

$$G_\theta^2 = 1 - \frac{\sqrt{3}\beta}{\alpha} \qquad (13)$$

---

[2]For the sake of simplicity we will drop the pixel coordinates (x,y) in the remaining of this section

where $\alpha = \|\Delta\|_2$ and $\beta = \frac{1}{3}\|\Delta\|_1$.

Putting a multiplier $\alpha(\alpha + \sqrt{3}\beta)$ to both sides of Eq. 13 yields:

$$\alpha(\alpha + \sqrt{3}\beta)G_\theta = \alpha^2 - 3\beta^2 \qquad (14)$$

Finally, combing Eq. 12 and 14 we obtain the sought relationship:

$$G_\sigma = \gamma G_\theta, \qquad (15)$$

where γ^2 equals to $\alpha(\alpha + \sqrt{3}\beta)/3\upsilon$.

From Eq. 15 it is clear that the original grayness function $G_\sigma(x,y)$ contains not only the real grayness – cosine distance $G_\theta(x,y)$ from the gray light – but also introduces a non-linear luminance-dependent term $\gamma(x,y)$, which adds noise to the grayness estimate. As a result, two points with same values of $G_\theta(x,y)$ but different luminance values will yield different values of $G_\sigma(x,y)$. In contrast, the proposed grayness function $G_\theta(x,y)$ is more robust to changes in luminance.

After some post-processing steps (*e.g.* local averaging and normalization by image intensity), a small percentage of pixels (*N%*) with the highest grayness values (lowest *G*) are chosen and averaged to be the illumination estimate. However, as it will be shown in the next section, the chosen gray pixels may still contain a number of colorful pixels. As a result, we will apply Mean Shift clustering in 3D RGB space in order to remove spurious color pixels. In the experiments in the remaining of this paper, we will use the new grayness function unless indicated otherwise.

4.3 Mean Shift Purification

Let *S* be the set of preselected *N%* pixels according to their grayness levels. Ideally, *S* should only contain pure-gray pixels. However, in fact *S* may contain a number of colorful pixels that need to be removed before estimating the global illumination of the scene.

In order to remove color pixels from *S*, we note that, for a color-biased image *I*, all the pure-gray pixels should be contained in the illumination direction $[L_r, L_g, L_b]$. This is equivalent to having all the pixels aligned towards the gray-light vector $\mathbf{g} = [1,1,1]^\intercal$ in the canonical image. For illustration purposes, Fig. 3j shows all the pixels of the canonical image of Fig. 3g in RGB space and Fig. 3k shows the corresponding set *S* of pre-selected gray-pixels. From Fig. 3k, it is clear that *S* contains both color and gray pixels. As predicted by our assumption, most true-gray pixels are aligned towards one single direction. In particular, the main direction of the densest pixel cloud indicates the illumination of the scene.

In this paper, we use *mean shift* (MS) clustering (Fukunaga and Hostetler, 1975; Comaniciu and Meer, 2002) with a hybrid distance to seek for the dark-to-bright elongated cluster which contains the most pixels in *S*. MS is a non-parametric space analysis algorithm, treating the feature space as a probability density function and seeking for the modes. In this work, the density of each pixel $p \in S$ in RGB space is calculated as a function of the bandwidth *h*:

$$\hat{f}(p) = \frac{1}{n}\sum_{i=1}^{n} K(p, p_i; h), \qquad (16)$$

where *n* the number of pixels in *S*, and the kernel density function $K(\cdot)$ is defined as:

$$K(p, p_i; h) = \begin{cases} 1, & \text{if } D(p, p_i) \leq h \\ 0, & \text{otherwise} \end{cases} \qquad (17)$$

with $\mathbf{I}(p) = [I_r, I_g, I_b]$ being the vector with RGB values of pixel *p*, $D(p, p_i)$ is the defined hybrid distance computed as the product of the euclidean and angular distances $\|\mathbf{I}(p) - \mathbf{I}(p_i)\|_2 \cdot \angle\{\mathbf{I}(p), \mathbf{I}(p_i)\}$, and $\angle\{\cdot\}$ is the angle between two vectors.

Finally, the centroid corresponding to the mode with highest density is used for the computation of the illumination estimate:

$$\hat{L} = \arg\max_{p \in S} \hat{f}(p). \qquad (18)$$

The effect of mean shift clustering on the detection of gray pixels is illustrated in Fig. 3. Comparing Figs. 3h and 3i, it is clear how the mean-shift clustering, simply and effectively, allows for the detection and removal of color pixels in the initial set *S*. It is worthy to mention that, in some cases, there is almost no colored pixels in *S*. Fortunately, the performance will not suffer from clustering, as MS gracefully generates only one cluster which gives us a reliable estimate. As a result, there is no need to condition when to apply clustering.

The mean-shifted gray pixel algorithm (MSGP) is summarized in Algorithm 1. The proposed method depends only in two parameters: the percentage of pixels chosen from their grayness values, *N%*, and the clustering bandwidth *h* of Eq. 16. The selection of these parameters and their effect on the performance of the proposed MSGP algorithm are presented in section 5.3.

5 EXPERIMENTS

Experiments were conducted in two widely known, publicly available datasets collected for the purpose of evaluation of color constancy methods:
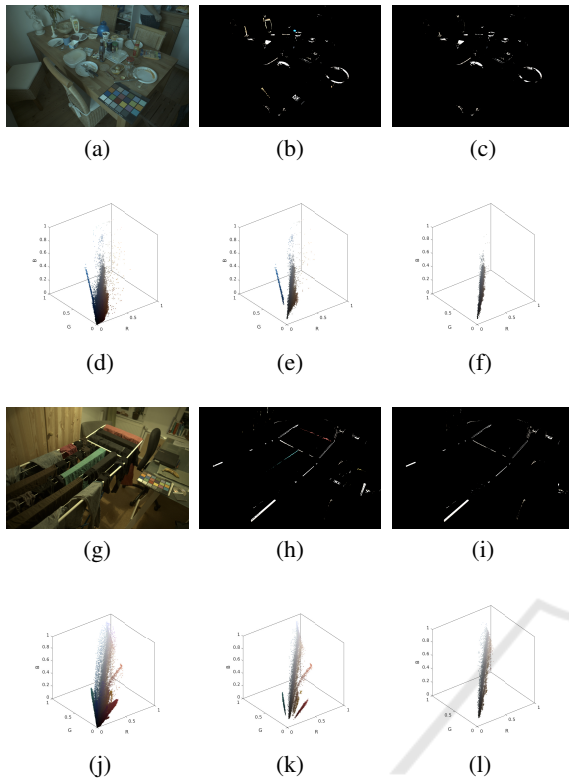
Figure 3: Detection of gray pixels. After correction using ground-truth illumination, ideal gray pixel should looks purely gray. (a,g) Input image, (b,h) Initial gray pixels detected. (c,i) Purified gray pixels after the Mean Shift step. (d-f, j-l) color histograms of (a-c). Comparing (e) with (f), (j) with (l), it is clear that Mean Shift helps to discard color pixels in (e) that are not aligned with the main illumination vector. For visualization purposes, the luminance of (b,c) is multiplied by a constant 4.

- Gehler-Shi Dataset (Shi and Funt, 2010): 568 high dynamic linear images, 2 cameras [3].
- NUS 8-Camera Dataset (Cheng et al., 2014): 1736 high dynamic linear images, 8 cameras [4].

The parameters of the proposed MSGP algorithm were selected as follows: the local contrast operator used in Eq. 9 was the Laplacian of Gaussian with a range of 5 pixels. The bandwidth for MS clustering was set to $h = 0.001$. The percentage of pixels chosen for the generation of S was set to $N = 0.1\%$. These parameters were selected based on preliminary experiments (see Section 5.3) and remained fixed for all the experiments.

In order to allow for a rigorous comparison with state-of-the-art methods, we have considered two sce-

---

[3]cameras: Canon 1D, Canon 5D

[4]cameras: Canon 1DS Mark3, Canon 600D, Fujifilm X-M1, Nikon D5200, Olympus E-PL6, Panasonic Lumix DMC-GX1, Samsung NX2000, Sony SLT-A57

Algorithm 1: Mean-Shifted Gray Pixel.

Inputs:
   I ▷ Color-biased image
Parameters:
   N ▷ Percentage of pixels

   h ▷ Bandwidth for MS clustering
Output:
   $\hat{L}$ ▷ Estimated illumination.

Steps:
1. Compute local contrast $\Delta(x,y)$
2. Compute grayness measure $G_\theta(x,y)$.   ▷ Eq. 8
3. Generate S with the top-$N\%$ gray pixels.
4. MS clustering on S with bandwidth h.   ▷ Eq. 16
5. Select $\hat{L}$ as the strongest mode of $\hat{f}$.   ▷ Eq. 18

---

narios. The *camera-agnostic* setting and the *camera-known* setting. In the agnostic-camera setting, learning-based algorithms are trained in one dataset (e.g., Gehler-Shi) and tested on the other. This allows for testing the performance of the algorithm in cameras not previously "seen" in the training process. The camera-known setting corresponds to the typical 3-fold cross validation used in the literature, in which learning-based methods are trained and validated in the same dataset. Visual comparison is given in Fig. 1, where the proposed method detects gray pixels more accurately. Numerical statistics are summarized in Table 2 and discussed in Sections 5.2 and 5.1.

5.1 Camera-known Setting

Camera-known setting (also termed as single-dataset setting) is the most common setting in related works, allowing extensive pre-training using a k-fold validation for learning-based methods. The results for this setting are summarized in table 2b. Among all the compared methods, FFCC yields the best overall performance in both datasets. It is important to remark that, cross validation makes no difference in the performance of statistical methods. Therefore, in order to avoid repetition, the performance of competing statistical methods is not shown in this table (see next section). Remarkably, it is clear that, even in the known-camera setting, the proposed algorithm outperforms several learning-based methods (from Gamut (Gijsenij et al., 2010) to the Exemplar-based method (Joze and Drew, 2014)) without extensive training and parameter tuning.

5.2 Camera-agnostic Setting

In order to allow for a fair comparison in the camera-agnostic scenario, learning-based methods should be

Table 2: Comparison of color constancy methods. All values correspond to angular error in degrees. For (a,b) we retrieve the results of the related works in the following order: 1) the cited paper, 2) Table [1] and Table [2] from Barron *et al.* (Barron and Tsai, 2017; Barron, 2015) considered to be up-to-date and comprehensive, 3) the color constancy benchmarking website (Gijsenij, 1999). We left dash on unreported results. In (b) results of learning-based methods worse than ours are marked in gray. The training time and testing time are reported in seconds, averagely per image, if reported in the original paper.

(a) Camera-agnostic setting

Training set	NUS 8-Camera					Gehler-Shi					Average	
Testing set	Gehler-Shi					NUS 8-Camera					runtime (s)	
	Mean	Median	Trimean	Best 25%	Worst 25%	Mean	Median	Trimean	Best 25%	Worst 25%	Train	Test
Learning-based Methods (agnostic-camera setting), Our rerun												
Bayesian	4.75	3.11	3.50	1.04	11.28	3.65	3.08	3.16	1.03	7.33	764	97
Chakrabarti *et al.* 2015 Empirical	3.49	2.87	2.95	0.94	7.24	3.87	3.25	3.37	1.34	7.50	–	0.30
Chakrabarti *et al.* 2015 End2End	3.52	2.71	2.80	0.86	7.72	3.89	3.10	3.26	1.17	7.95	–	0.30
Cheng *et al.* 2015	5.52	4.52	4.79	1.96	12.10	4.86	4.40	4.43	1.72	8.87	245	0.25
FFCC	3.91	3.15	3.34	1.22	7.94	3.19	2.33	2.52	0.84	7.01	98	0.029
Physics-based Methods												
IIC	13.62	13.56	13.45	9.46	17.98	–	–	–	–	–	–	–
Woo *et al.* 2018	4.30	2.86	3.31	0.71	10.14	–	–	–	–	–	–	–
Biological Methods												
Double-Opponency	4.00	2.60	–	–	–	–	–	–	–	–	–	–
ASM 2017	3.80	2.40	2.70	–	–	–	–	–	–	–	–	–
Statistical Methods												
White Patch	7.55	5.68	6.35	1.45	16.12	9.91	7.44	8.78	1.44	21.27	–	0.16
Grey World	6.36	6.28	6.28	2.33	10.58	4.59	3.46	3.81	1.16	9.85	–	0.15
General GW	4.66	3.48	3.81	1.00	10.09	3.20	2.56	2.68	0.85	6.68	–	0.91
2st-order grey-Edge	5.13	4.44	4.62	2.11	9.26	3.36	2.70	2.80	0.89	7.14	–	1.30
1st-order grey-Edge	5.33	4.52	4.73	1.86	10.43	3.35	2.58	2.76	0.79	7.18	–	1.10
Shades-of-grey	4.93	4.01	4.23	1.14	10.20	3.67	2.94	3.03	0.99	7.75	–	0.47
Grey Pixel (edge) [2]	4.60	3.10	–	–	–	3.15	2.20	–	–	–	–	0.88
LSRS	**3.31**	2.80	2.87	1.14	**6.39**	3.45	2.51	2.70	0.98	7.32	–	2.60
Cheng *et al.* 2014	3.52	2.14	2.47	0.50	8.74	2.93	2.33	2.42	0.78	**6.13**	–	0.24
Mean Shifted Gray Pixel	3.45	**2.00**	**2.36**	**0.43**	8.47	**2.92**	**2.11**	**2.28**	**0.60**	6.69	–	1.32

(b) Camera-known setting

	Gehler-Shi					NUS 8-camera				
	Mean	Median	Trimean	Best 25%	Worst 25%	Mean	Median	Trimean	Best 25%	Worst 25%
Learning-based Methods (camera-known setting)										
Edge-based Gamut	6.52	5.04	5.43	1.90	13.58	4.40	3.30	3.45	0.99	9.83
Pixel-based Gamut	4.20	2.33	2.91	0.50	10.72	5.27	4.26	4.45	1.28	11.16
Bayesian	4.82	3.46	3.88	1.26	10.49	3.50	2.36	2.57	0.78	8.02
Natural Image Statistics	4.19	3.13	3.45	1.00	9.22	3.45	2.88	2.95	0.83	7.18
Spatio-spectral (GenPrior)	3.59	2.96	3.10	0.95	7.61	3.06	2.58	2.74	0.87	6.17
Corrected-Moment[1] (19 Edge)	3.12	2.38	2.59	0.90	6.46	3.03	2.11	2.25	0.68	7.08
Corrected-Moment[1] (19 Color)	2.96	2.15	2.37	0.64	6.69	3.05	1.90	2.13	0.65	7.41
Exemplar-based [*]	2.89	2.27	2.42	0.82	5.97	–	–	–	–	–
Chakrabarti *et al.* 2015	2.56	1.67	1.89	0.52	6.07	–	–	–	–	–
Cheng *et al.* 2015	2.42	1.65	1.75	0.38	5.87	2.18	1.48	1.64	0.46	5.03
DS-Net (HypNet+SelNet)	1.90	1.12	1.33	0.31	4.84	2.24	1.46	1.68	0.48	6.08
CCC (dist+ext)	1.95	1.22	1.38	0.35	4.76	2.38	1.48	1.69	0.45	5.85
FC[4] (AlexNet)	**1.77**	1.11	1.29	0.34	**4.29**	2.12	1.53	1.67	0.48	4.78
FFCC	1.78	**0.96**	**1.14**	**0.29**	4.62	**1.99**	**1.31**	**1.43**	**0.35**	**4.75**
Mean Shifted Gray Pixel	3.45	2.00	2.36	0.43	8.47	2.92	2.11	2.28	0.60	6.69

[1] For Correct-Moment (Finlayson, 2013) we report reproduced and more detailed results by (Barron, 2015), which slightly differs with the original results:

mean: 3.5, median: 2.6 for 19 colors and mean: 2.8, median: 2.0 for 19 edges on Gehler-Shi Dataset.

[2] We rerun Grey Pixel (edge) on NUS dataset.

[*] We mark Exemplar-based method with asterisk as it is trained and tested on a uncorrected-blacklevel dataset.

re-trained for evaluation in the same conditions as statistical methods. Several state-of-the-art CNN-based methods are not publicly available. In this work, we were able to re-run the Bayesian method (Gehler et al., 2008), Chakrabarti *et al.*(Chakrabarti, 2015), FFCC (Barron and Tsai, 2017), and the method by Cheng *et al.* 2015 (Cheng et al., 2015), using the codes provided by the original authors. Note that this list of methods includes FFCC, which showed the best overall performance in the camera-known setting.

We train on one dataset and test on the other one. Both datasets share no common cameras, thus meeting our requirement of being "camera-agnostic". For the results reported in this section, we use the best or final setting for each method: Bayes (GT) for Bayesian; Empirical and End-to-End training for Chakrabarti *et al.* (Chakrabarti, 2015); 30 regression trees for Cheng *et al.*; full image resolution and 2 chan-

Table 3: Comparison between Mean Shift Clustering vs. K-means Clustering in our task. "angle" refers to using angular distance only in Mean Shift instead of the proposed hybrid distance.

	SFU Color Checker			NUS 8-Camera		
	Mean	Med	Trimean	Mean	Med	Trimean
Mean Shift						
h=1e−3 (angle)	3.62	2.08	2.42	3.00	2.10	2.26
h=1e−4	3.51	2.04	2.38	3.32	2.13	2.39
h=1e−3	3.45	2.00	2.36	2.92	2.11	2.28
h=1e−2	3.48	2.11	2.44	3.00	2.19	2.39
Kmeans						
K=2	3.75	2.18	2.54	3.00	2.10	2.28
K=5	4.44	2.46	2.73	3.32	2.13	2.37
K=9	4.50	2.51	2.80	3.37	2.19	2.39

nels for FFCC[5]. Obtained results are summarized in Table 2a.

Obtained results are summarized in Table 2a. From this table, it is clear that the proposed MSGP algorithm outperforms both learning-based and statistical methods. Except FFCC, selected learning-based methods perform relatively worse in camera-agnostic setting, as compared to statistical methods. Due to their nature, it is not surprising that learning-based methods degrade in their performance in the camera-agnostic scenario. However, the fact that learning-based methods are outperformed by statistical methods is an interesting finding. On one side, if we use learning-based methods trained for a given dataset or "a bag of camera models", we may fail in the camera-agnostic setting. In contrast, in the both camera-agnostic/known setting, the proposed statistical method provides stable performance.

5.3 Algorithm Parameters

The Role of Bandwidth h. The bandwidth h determines the domain size where Mean Shift computes the pixel divergence. Here we evaluate variants of the proposed method by changing h to be 1e−4, 1e−3 and 1e−2. Table 3 shows that the bandwidth 1e−3 gives a good trade-off between mean and median error on two datasets. For reference purposes, Table 3 also includes performance results obtained when the distance function in Eq. 17 uses only angular information in $D(\cdot)$.

Clustering Algorithm. We compare two clustering methods, Mean Shift and K-means[6]. Here we evaluate variants of K-means by changing the number of clusters K to 2, 5 and 9. Table 3 shows that, in general, MS gives better results. This can be attributed to the

---

[5]Scripts for re-running these methods will also be public.

[6]We use clustering to find the mode *i.e.* the dominating illumination color, while we don't need all all clustered indexes. We note that other clustering methods (*e.g.* spectral clustering) may work well. We selected Mean Shift due to its fast computation and robustness to the outliers.

fact that Mean Shift is more robust to outliers than K-means. Among all K-means invariants, the 2-cluster setting performs best. This suggests that S usually contains $1 - 2$ elongated clusters.

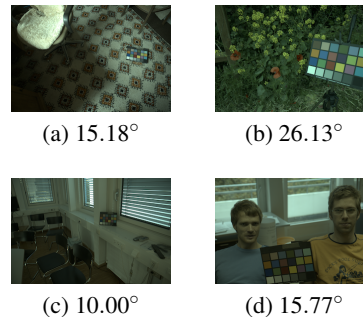(a) 15.18° (b) 26.13°

(c) 10.00° (d) 15.77°

Figure 4: Example failure cases with their angular errors. (a,b) are examples with no detectable gray pixels (note that the ground truth color chart is masked in evaluation). (c,d) are examples with mixed illumination: indoor illumination and outdoor illumination.

6 LIMITATIONS AND CONCLUSIONS

Our method relies on gray pixels and their statistics for one global illumination estimation. Therefore, in some extreme cases, when there are no detectable gray pixels or there are gray pixels representing two not-same-color illuminations, our method fails. In Figure 4, two no-gray-pixel examples and two double-illumination examples are shown. Cheng *et al.* (Cheng et al., 2016) claimed that in SFU Color Checker Dataset (Shi and Funt, 2010), there are 66 two-illumination images (image list released). It is worthy to mention that the images where we fail overlap largely with this two-illumination list. As mixed-illumination problem is a different task and out of the scope of this paper, we refer readers to (Cheng et al., 2016) for details.

In this paper, we presented a statistical method for tackling the problem of color constancy. The proposed method relies on gray pixel detection and mean shift clustering in order to estimate the illumination of the scene based on the statistical properties of the gray pixels of the input image. In the camera-agnostic scenario, in which color constancy is to be applied to images captured with unknown cameras, the proposed method outperforms both learning-based and statistical state-of-the-arts.

The proposed method is easy to implement, training-free, and depends only on two parameters, namely the percentage of gray pixels $N\%$ and the

Mean Shift bandwidth h. With our method, processing a 2000×1500 linear RGB image takes about 1.32 seconds with unoptimized MATLAB code running in a CPU Intel i7 2.5 GHz. The method can be adapted to other color spaces (*e.g.* Lab) without any performance drop.

REFERENCES

Barnard, K., Cardei, V., and Funt, B. (2002). A comparison of computational color constancy algorithms. i: Methodology and experiments with synthesized data. *TIP*, 11(9):972–984.

Barron, J. T. (2015). Convolutional color constancy. In *ICCV*.

Barron, J. T. and Tsai, Y.-T. (2017). Fast fourier color constancy. In *CVPR*.

Brainard, D. H. and Wandell, B. A. (1986). Analysis of the retinex theory of color vision. *JOSA A*, 3(10):1651–1661.

Buchsbaum, G. (1980). A spatial processor model for object colour perception. *Journal of the Franklin Institute*, 310(1):1–26.

Chakrabarti, A. (2015). Color constancy by learning to predict chromaticity from luminance. In *NIPS*.

Chakrabarti, A., Hirakawa, K., and Zickler, T. (2012). Color constancy with spatio-spectral statistics. *TPAMI*, 34(8):1509–1519.

Cheng, D., Kamel, A., Price, B., Cohen, S., and Brown, M. S. (2016). Two illuminant estimation and user correction preference. In *CVPR*.

Cheng, D., Prasad, D. K., and Brown, M. S. (2014). Illuminant estimation for color constancy: why spatial-domain methods work and the role of the color distribution. *JOSA A*, 31(5):1049–1058.

Cheng, D., Price, B., Cohen, S., and Brown, M. S. (2015). Effective learning-based illuminant estimation using simple features. In *CVPR*.

Comaniciu, D. and Meer, P. (2002). Mean shift: A robust approach toward feature space analysis. *TPAMI*, 24(5):603–619.

Finlayson, G. D. (2013). Corrected-moment illuminant estimation. In *ICCV*, pages 1904–1911.

Finlayson, G. D. and Schaefer, G. (2001a). Convex and non-convex illuminant constraints for dichromatic colour constancy. In *CVPR*, volume 1, pages I–I. IEEE.

Finlayson, G. D. and Schaefer, G. (2001b). Solving for colour constancy using a constrained dichromatic reflection model. *IJCV*, 42(3):127–144.

Finlayson, G. D. and Trezzi, E. (2004). Shades of gray and colour constancy. In *Color Imaging Conference (CIC)*.

Foster, D. H. (2011). Color constancy. *Vision research*, 51(7):674–700.

Fukunaga and Hostetler (1975). The estimation of the gradient of a density function, with applications in pattern recognition. *IEEE Transactions on Information Theory*, 21:32–40.

Gao, S., Han, W., Yang, K., Li, C., and Li, Y. (2014). Fefficient color constancy with local surface reflectance statistics. In *ECCV*.

Gao, S.-B., Zhang, M., Li, C.-Y., and Li, Y.-J. (2017). Improving color constancy by discounting the variation of camera spectral sensitivity. *JOSA A*, 34(8):1448–1462.

Gehler, P. V., Rother, C., Blake, A., Minka, T., and Sharp, T. (2008). Bayesian color constancy revisited. In *CVPR*.

Geusebroek, J.-M., Van den Boomgaard, R., Smeulders, A. W. M., and Geerts, H. (2001). Color invariance. *TPAMI*, 23(12):1338–1350.

Gijsenij, A. (1999). Color constancy research website: http://colorconstancy.com.

Gijsenij, A. and Gevers, T. (2011). Color constancy using natural image statistics and scene semantics. *TPAMI*, 33(4):687–698.

Gijsenij, A., Gevers, T., and Van De Weijer, J. (2010). Generalized gamut mapping using image derivative structures for color constancy. *IJCV*, 86(2-3):127–139.

Gijsenij, A., Gevers, T., and Van De Weijer, J. (2011). Computational color constancy: Survey and experiments. *TIP*, 20(9):2475–2489.

Hu, Y., Wang, B., and Lin, S. (2017). Fully convolutional color constancy with confidence-weighted pooling. In *CVPR*.

Joze, H. R. V. and Drew, M. S. (2014). Exemplar-based color constancy and multiple illumination. *TPAMI*, 36(5):860–873.

Qian, Y., Chen, K., Kämäräinen, J., Nikkanen, J., and Matas, J. (2016). Deep structured-output regression learning for computational color constancy. In *ICPR*.

Qian, Y., Chen, K., Kämäräinen, J., Nikkanen, J., and Matas, J. (2017). Recurrent color constancy. In *ICCV*.

Shi, L. and Funt, B. (2010). Re-processed version of the gehler color constancy dataset of 568 images. *accessed from http://www.cs.sfu.ca/ colour/data/*.

Shi, W., Loy, C. C., and Tang, X. (2016). Deep specialized network for illumination estimation. In *ECCV*.

Tominaga, S. (1996). Multichannel vision system for estimating surface and illumination functions. *JOSA A*, 13(11):2163–2173.

Van De Weijer, J., Gevers, T., and Gijsenij, A. (2007). Edge-based color constancy. *TIP*, 16(9):2207–2214.

von Kries, J. (1970). Influence of adaptation on the effects produced by luminous stimuli. *Source of Color Science*, pages 109–119.

Woo, S.-M., Lee, S.-h., Yoo, J.-S., and Kim, J.-O. (2018). Improving color constancy in an ambient light environment using the phong reflection model. *TIP*, 27(4):1862–1877.

Xiong, W., Funt, B., Shi, L., Kim, S.-S., Kang, B.-H., Lee, S.-D., and Kim, C.-Y. (2007). Automatic white balancing via gray surface identification. In *Color and Imaging Conference (CIC)*.

Yang, K.-F., Gao, S.-B., and Li, Y.-J. (2015). Efficient illuminant estimation for color constancy using grey pixels. In *CVPR*.

APPENDIX

Detailed Settings of Learning-based Methods

To evaluate the performance of learning-based method in camera-agnostic scenario, we re-run the Bayesian method (Gehler et al., 2008), Chakrabarti *et al.* 2015 (Chakrabarti, 2015), FFCC (Barron and Tsai, 2017), and the method by Cheng *et al.* 2015 (Cheng et al., 2015), using the codes provided by the authors. FFCC shows the best overall performance in the camera-known setting. Our experimental settings for re-running the aforementioned algorithms are summarized below:

Bayesian method (Gehler et al., 2008)	Among all variations of Bayesian methods stated in (Gehler et al., 2008), we use Bayes (GT) but without indoor/outdoor split, to which Bayes (tanh) is sensible. The ground truth of training illuminations (*e.g.* Gehler-Shi) is used as point-set prior for testing on the other dataset (*e.g.* NUS 8-camera)
Chakrabarti *et al.* 2015 (Chakrabarti, 2015)	We use both variations given by the author: the empirical and the end-to-end trained method. We keeps all training hyperparameters same, *e.g.* epoch number, momentum and learning-rate for SGD.
FFCC (Barron and Tsai, 2017)	For fair comparison, we use Model (J) (FFCC full,4 channels) in (Barron and Tsai, 2017), which is free of camera metadata and semantic information but still state-of-the-art.
Cheng *et al.* 2015 (Cheng et al., 2015)	Same as (Cheng et al., 2015), we use four 2D features with an ensemble of regression trees (K=30).